

Articles

End-Group Cross-Linked Poly(arylene ether) for Proton Exchange Membranes

Kwan-Soo Lee, Myung-Hwan Jeong, Jung-Pil Lee, and Jae-Suk Lee*

Department of Materials Science and Engineering and Center for Advanced Materials Research and Education, Gwangju Institute of Science and Technology, 261 Cheomdan-gwagiro (Oryong-dong), Buk-gu, Gwangju 500-712, Republic of Korea

Received October 9, 2008; Revised Manuscript Received December 6, 2008

ABSTRACT: End-group cross-linkable sulfonated poly(arylene ether) polymer (E-SFQK) was synthesized via direct polymerization of potassium 2,5-dihydroxybenzenesulfonate (SHQ) and decafluorobiphenyl (DFBP), followed by a reaction with ethynylphenol (EP). The cross-linking reaction of the ethynyl end group of E-SFQK was performed at 250 °C. After cross-linking, proton conductivity, water uptake, and swelling ratio of cross-linked membrane decreased from 0.16 (noncross-linked membrane) to 0.13 S/cm, from 86% to 42%, and from 31% to 13%, respectively. The effect of cross-linking time on proton conductivity, water uptake, and swelling ratio were also investigated. Methanol permeability of cross-linked membrane was compared with Nafion 117 due to solubility of noncross-linked membranes in methanol. The cross-linked membrane performed better, with a methanol permeability of 88×10^{-8} cm²/s, as compared with 154×10^{-8} cm²/s for Nafion 117. The cross-linked membrane also exhibited improved chemical resistance and oxidative stability from solubility and Fenton's tests. In order to study morphological changes of cross-linked and noncross-linked membranes, hydrophilic domain sizes from an AFM phase image were evaluated. These results showed that the sizes of hydrophilic domains of the cross-linked membrane (5–20 nm) are much smaller than those of noncross-linked membrane (20–50 nm).

Introduction

Polymer electrolyte membrane fuel cells (PEMFCs) have attracted a great deal of attention as alternative and environmentally friendly energy sources for transportation, portable devices, and stationary power.¹ Polymer electrolyte membranes require high proton conductivity, sufficient thermal stability, low permeability to fuel and oxidant, and long-term stability and durability.² Perfluorinated sulfonic acids (PFSA)s such as Nafion, which have excellent proton conductivity, good mechanical and chemical properties, and long-term durability, are commonly used as polymer electrolytes for PEMFCs. However, the membranes are not appropriate for high temperature use due to their low glass transition temperature (ca. 110 °C), which induces decreased proton conductivity and mechanical properties. Moreover, their cost and complicated synthesis procedure are critical drawbacks.^{2,3}

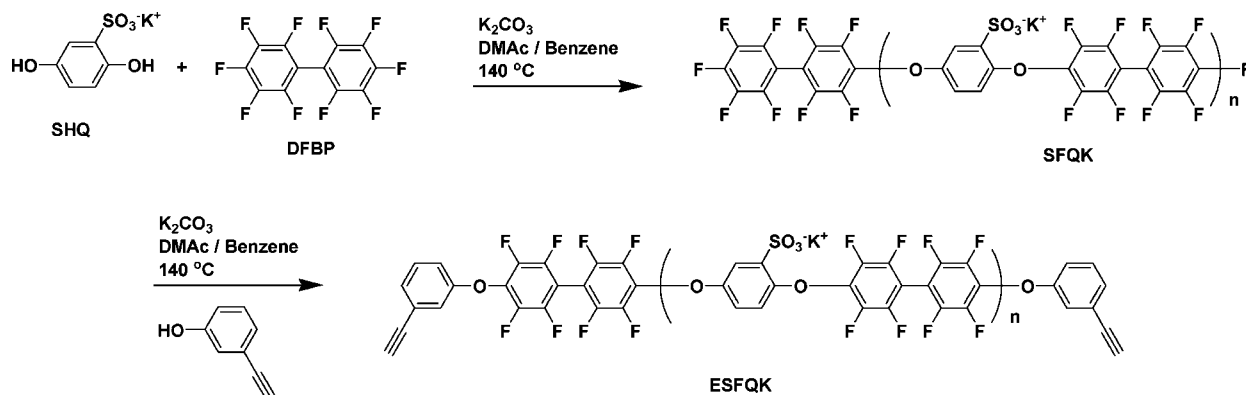
As an effective alternative, sulfonated aromatic polymers,^{1a,2,3c} such as poly(arylene ether)s,⁴ poly(arylene ether ether ketone)s,⁵ polyimides,⁶ poly(phenylene sulfide)s,⁷ poly(*p*-phenylene)s,⁸ and polybenzimidazoles⁹ have been investigated as PEM materials. Although these polymers have their own advantages, such as good proton conductivity, thermal stability, and low cost, most of them have a crucial problem of deficient long-term durability under high operating temperatures of fuel cells. General problems of long-term durability are diffusion of oxygen molecules through the membrane and incomplete reduction, generating active radicals on the platinum catalyst, which can attack the membrane material.¹⁰ The dominating reaction of degradation processes is the addition reaction of HO•

to the aromatic rings of phenyl containing polymers, especially in the *ortho* position to alkyl and ether linkage (–O–).¹¹ This demonstrates the combined *ortho* activation by these substituents and the *meta*-directing effect of the SO₃ group in electrophilic addition reactions. Consequently, there has been extensive interest in the development of ionomer membrane materials that retain long-term durability from the radical attack while possessing reasonable transport properties.

Many researchers have studied fluorinated aromatic polymers containing sulfonic acid groups¹² to improve long-term durability of membranes with high proton conductivity. C–F bonds are stronger than C–H bonds, which can prevent degradation by HO• and HO₂• radicals, and which causes unique properties of fluorine-containing polymers such as excellent thermal and oxidative stability, chemical inertness, good surface properties, low moisture absorption, good film-forming property, and easy processability compared with nonfluorinated hydrocarbon aromatic polymers.^{10,11,13} Watanabe group has observed the membrane containing trifluoromethyl group undergo radical attack using Fenton's test under very harsh conditions (3% H₂O₂ aqueous solution containing 2 ppm FeSO₄ at 80 °C).^{12a} In the study, the effect of hydrophobic groups on prolonging the dissolution time was investigated with a branched polymer membrane. It was seen that hydrophobic domains consisting of fluorine groups not only contribute to increasing the hydrophilic-hydrophobic phase separation of the ionomer, but also easily stabilize the sulfonate groups (SO₃[–]) when they dissociate because fluorine groups have a high electronegativity, increasing the electron withdrawing effect. In order to increase hydrophobicity and thermal, mechanical, and chemical stabilities, fluorinated components such as decafluorobiphenyl and trifluoro-

* Corresponding author. E-mail: jslee@gist.ac.kr.

Scheme 1. Synthesis of SFQK and E-SFQK



methyl moieties have been introduced into the polymer main chain and side chain, respectively.^{12a–d} More recently, McGrath and co-workers have reported hydrophilic–hydrophobic multi-block copolymers for PEMs with a highly phase-separated morphology.^{12e}

Cross-linking of polymer membrane was also deemed to be an important prerequisite to alleviate and to overcome the long-term durability problem. In a recent review, Kerres has introduced two types of cross-linked membranes, summarizing with detailed property comparisons.¹⁴ However, these reviews posited that ionic acid–base ionomer membranes and covalently cross-linked membranes suffer from deteriorating dimensional and mechanical properties in $70\text{ }^\circ\text{C}$ water¹⁵ and reduction of the IEC of the membranes after elimination of sulfonic acid groups, which were involved in the cross-linking reaction, thus giving decreasing the proton conductivity of the membrane.¹⁶ respectively. Very few reports have presented covalently cross-linking ionomer membranes without elimination of sulfonic acid groups. Watanabe group introduced a trifunctional monomer for branching or cross-linking into the polymer main chain.^{12a,17} Zhong and Heo prepared photochemically cross-linkable aromatic membranes containing a double bond ($C=C$) for photo-cross-linking into the side chain and main chain of the polymers.¹⁸ In our work, to achieve high proton conductivity without elimination of the sulfonic acid group (which would induce low IEC values) during cross-linking and without addition of chemical additives and impurities for the cross-link reaction, a covalently thermal-cross-linkable end group system was proposed.

Several important factors, such as membrane treatment method, morphology, molecular composition of the membrane, degree of sulfonation, and polarity of the membrane, influence the transport properties of the polymer electrolyte membrane. The McGrath group has studied the effect of acidification on morphology, which affects water uptake, conductivity, methanol permeability, and stability of the sulfonated poly(arylene ether sulfone) copolymer.^{4c,d} The morphological effects on transport properties of PEM were further investigated by alternating chemical composition^{4e} and copolymer architecture.^{4f} Cross-linking the polymer also affects the polymer structure. In an earlier study, the McGrath group also reported the structural change of the cross-linkable polymer after cross-linking, with high thermal stability.¹⁹ However, there has been little study into the field of polymer electrolytes for fuel cells, especially sulfonated polymers without elimination of the sulfonic acid group for cross-linking with morphological study.

In this study, we present the synthesis of a new ethynyl-terminated sulfonated-fluorinated poly(arylene ether) ionomer with the aim of achieving three main attributes: sufficient oxidative stability to withstand typical degradation from attack-

ing HO^\bullet and HO_2^\bullet radicals that originate from oxygen diffusion through the membrane and incomplete reduction at the fuel cell anode;¹⁰ low water uptake and swelling of the membrane, which cause the loss of dimensional stability and mechanical strength; and low fuel crossover with excellent proton conductivity. For the ionomer to meet the above demands, a high fluorinated monomer (decafluorobiphenyl) was used to prepare the ionomer. Furthermore, an ethynyl moiety at the end of the polymer as the thermal-cross-linkable group was introduced not only to increase thermo-oxidative stability, chemical resistance, and dimensional stability, but also to achieve reasonable proton conductivity without decreasing the IEC value of membrane.

Experimental Section

Materials. Potassium 2,5-dihydroxybenzenesulfonate (SHQ) and potassium carbonate were purchased from Aldrich Chemical Co. and used after vacuum drying at $100\text{ }^\circ\text{C}$ for 2 days. Benzene and *N,N*-dimethylacetamide (DMAc) were purchased from Aldrich Chemical Co. and used without further purification. Decafluorobiphenyl (DFBP) was purchased from Fluorochem Ltd. and used without purification. 3-Ethynylphenol was prepared according to the literature.^{13c}

Synthesis of SFQK and E-SFQK. Sulfonated-fluorinated poly(arylene ether) (SFQK) was synthesized via step growth polymerization of SHQ with DFBP as shown in Scheme 1. SHQ (4.57 g, 20.0 mmol) and DFBP (6.70 g, 1.002 equiv) with K_2CO_3 (3.40 g, 1.15 equiv) were dissolved in a DMAc (60 mL) and benzene (20 mL) mixture and placed in a 250 mL, 2-neck flask equipped with a magnetic stirrer, a nitrogen inlet, and a Dean–Stark trap. The reaction mixture was heated to $140\text{ }^\circ\text{C}$, and this temperature was maintained for 12 h to ensure complete dehydration. Benzene was refluxed into the Dean–Stark trap, following which the reaction mixture was stirred at this temperature for a further period of 2 h. After removing benzene, the reaction mixture was stirred at this temperature for a further period of 2 h. To synthesize E-SFQK, the end of the SFQK was capped by an ethynyl group. In a typical procedure for attaching the ethynyl group at the end of polymer, 3-ethynylphenol (0.40 g, 0.17 eq.), DMAc (20 mL), and benzene (10 mL) were added to the reaction mixture, and the reaction was continued for another 3 h. The reaction mixture was cooled and precipitated into 1 L of ethanol/water (9.8:0.2 solution). The precipitated polymer was filtered and washed with ethanol. The brown solid was dried under vacuum ($60\text{ }^\circ\text{C}$) for 3 days. The combined yield of SFQK and E-SFQK was above 90%.

E-SFQK. ^1H NMR ($\text{DMSO}-d_6$): $\delta = 7.53$ (1H, s, SHQ moiety), 7.31 (1H, s, SHQ moiety), 7.28 (1H, s, SHQ moiety), 7.15–6.99 (br, phenyl ring at polymer end group), 4.17 (s, ethynyl moiety at polymer end group). ^{19}F -NMR ($\text{DMSO}-d_6$): $\delta = -136.12$ (4F, dd), -151.58 (4F, dd). IR (KBr, cm^{-1}): 1019 (sym, $-\text{SO}_3^-$), 1227 (asym, $-\text{SO}_3^-$), 1264 (wagging, $-\text{SO}_3^-$). Anal. Calcd for $(\text{C}_{18}\text{H}_3\text{F}_8\text{KO}_5\text{S})_n$: C, 41.39; H, 0.58; S, 3.73. Found: C, 41.47; H, 0.57; S, 3.70.

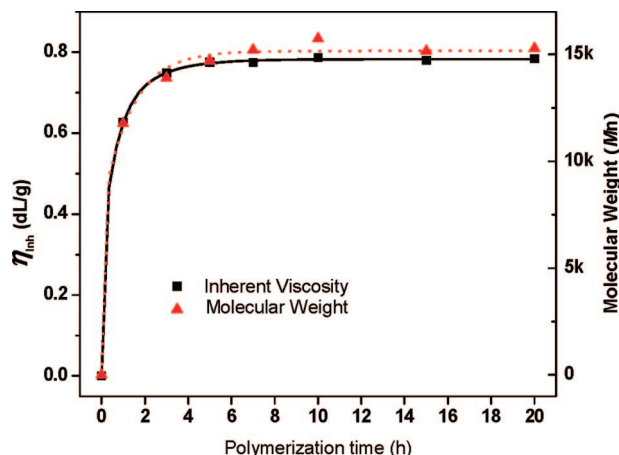


Figure 1. Effect of reaction time on the inherent viscosities (η_{inh}) and molecular weight (M_n) of E-SFQK.

Characterization and Measurements. *Nuclear Magnetic Resonance (NMR) Spectroscopy.* ^1H and ^{19}F NMR spectra were measured on a JEOL JNM-LA 300 WB FT-NMR in deuterated DMSO ($\text{DMSO}-d_6$). Chemical shifts of ^1H and ^{19}F NMR spectra were referenced to tetramethylsilane (TMS) at 0 ppm as an internal reference and fluorinated trichlorofluoromethane at 0 ppm as an external reference, respectively.

Fourier Transform Infrared (FT-IR) Spectroscopy. FT-IR spectroscopy was utilized to confirm the functional groups of the synthesized polymer. Measurements were conducted on a Perkin-Elmer IR 2000 series.

Thermal Analysis. The thermal properties of resulting membranes were determined with a TA Instrument 2100 series, covering the thermal degradation temperature range of 40–800 °C at a heating rate of 10 °C/min. Glass transition temperatures (T_g) of membranes were measured in the range of 40–350 °C at a heating rate of 5 °C/min using the differential scanning calorimeter (DSC) measurement.

Inherent Viscosity Determinations. The measurements of inherent viscosities (η_{inh}) of sulfonated polymers were performed using an Ubbelohde viscometer, thermostatically controlled in a water bath. Inherent viscosities (η_{inh}) were measured at 25 °C in DMAc. Inherent viscosities provide information on the size of a polymer molecule in solution. Typically, the inherent viscosity provides a qualitative inference of molecular weight. Inherent viscosities were very important in this dissertation because GPC could not be effectively used for sulfonated copolymers.

Low Temperature Stability Test. Hydrated and dried membranes were allowed to equilibrate by exposure to 100% relative humidity at room temperature for at least 10 days and by vacuum at 80 °C for 3 days, respectively. The low temperature tests at −30 °C were performed after storage in a refrigerator at −30 °C for 2 days. The membranes were then bent immediately at ambient conditions.

Chemical Resistance (Solubility Test) and Oxidative Stability. Chemical resistance was measured by using a solubility test of the membranes in various common organic solvents. All membranes were immersed in various common organic solvents for 24 h at room temperature. Oxidative stability was examined by immersing the membrane samples in Fenton's reagent (3% H_2O_2 aqueous solution containing 2 ppm FeSO_4) at 80 °C.^{12a}

Atomic Force Microscope (AFM). AFM images were acquired with a Nanoscope IIIa (Digital Instruments Inc., Santa Barbara,

CA). Super Sharp Silicon tapping mode with a cantilever resonance frequency of ca. 330 kHz was used (NanoSensors, Wetzlar-Blankenfeld, Germany). The tip of the cantilever had a nominal radius of curvature of ca. 2 nm. Scan rates of 0.5 Hz were used. All treated samples were allowed to equilibrate by exposure to 100% relative humidity at room temperature for at least for 24 h before testing. The samples were then imaged immediately at ambient condition.

Ion-Exchange Capacity. Ion-exchange capacity (IEC) was determined using the classical titration method. After acidifying and washing the membranes, they were immersed into 0.1 M NaCl solution for 24 h to replace H^+ with Na^+ . The remaining liquid was titrated with 0.1 M NaOH solution using phenolphthalein as an indicator. The IEC values were expressed as mequiv of ($-\text{SO}_3\text{H}$)/g of dry polymer and were obtained by the following equation:

$$\text{IEC (mequiv/g)} = \frac{\text{consumed NaOH} \times \text{molarity NaOH}}{\text{weight of dried membrane}}$$

Water Uptake and Swelling Ratio. Water uptake and swelling ratio were determined for all membranes in their acid forms. The acid-form membranes were dried at 80 °C under vacuum until a constant weight was recorded. They were then immersed in deionized water at 25 °C and periodically weighed on an analytical balance until constant water uptake weights were obtained. Typically, the equilibrium water sorption occurred within 72 h. The water uptake was calculated from a percentage of weight difference between wet membrane (W_{wet}) and dried membrane (W_{dry}) and dividing by the dry membrane (W_{dry}) weight. The swelling ratio was calculated from a percentage of length difference between wet membrane (l_{wet}) and dried membrane (l_{dry}) and dividing by the dry membrane (l_{dry}) length. The equations of water uptake (%) and swelling ratio (%) are given below:

$$\text{water uptake} = \frac{W_{wet} - W_{dry}}{W_{dry}} \times 100,$$

$$\text{swelling ratio} = \frac{l_{wet} - l_{dry}}{l_{dry}} \times 100$$

Proton Conductivity. A four-point probe method was used to measure the proton conductivity of the membranes. Before the measurement of proton conductivity, the prepared membranes were equilibrated with deionized water. Proton conductivity was performed by an impedance analyzer (AutoLab, PGSTAT 30, Netherlands) over the frequency range from 1 Hz to 1 MHz at 30 and 90 °C with a four-point probe method. Each membrane sample was cut in $4 \times 1 \text{ cm}^2$ prior to mounting on the cell, and was equilibrated with deionized water for 24 h. The proton conductivity was calculated by the equation below:

$$\sigma = \frac{L}{R \cdot S}$$

where σ (S/cm or $\Omega^{-1}\text{cm}^{-1}$) is proton conductivity, L (cm) is the distance between two electrodes used, R (Ω) is the resistance of the membrane, and S (cm^2) is the surface area for ions to penetrate the membrane. The impedance of each sample was measured at least five times to ensure data reproducibility.

Methanol Permeability. The methanol permeability of the membranes was determined using a diffusion cell. This cell consisted of two reservoirs, each with a capacity of approximately 150 mL, separated by a vertical membrane. Prior to the test, the membranes

Table 1. Solubility of E-SFQK, NSFQK, and CSFQK in Various Common Organic Solvents^a

sample ^b	NMP ^c	DMAc ^d	DMSO ^e	DMF ^f	THF ^g	acetone	CHCl_3	MeOH ^h	water
E-SFQK	S	S	S	S	I	I	I	P	I
NSFQK	S	S	S	S	P	P	Sw	S	I
CSFQK	I	I	I	I	I	I	I	I	I

^a S = soluble at room temperature, P = partially soluble at room temperature, I = insoluble at room temperature, Sw = swelling at room temperature. ^b E-SFQK: just dried polymer after polymerization (K^+ form), CSFQK: cross-linked membrane (H^+ form), NSFQK: noncross-linked membrane (H^+ form). ^c NMP: *N*-methylpyrrolidone. ^d DMAc: *N,N*-dimethylacetamide. ^e DMSO: dimethylsulfoxide. ^f DMF: dimethylformamide. ^g THF: tetrahydrofuran. ^h MeOH: methanol.

were equilibrated in deionized water for at least 24 h. The membrane was placed between two compartments: one filled with deionized water and the other filled with a 2 M methanol/water solution. The temperature of the diffusion cell was maintained at 25 °C with a water bath, and both compartments were stirred continuously during the experiments. The methanol concentration in the deionized water compartment was monitored with time using a refractive index detector (RI750F, Younglin Instrument Co., Korea) through a 1 mm diameter silicon tube with 1.0 mL/min constant speed driven by a Masterflex pump. The output signal was converted by a data module (Autochro, Younglin Instrument Co., Korea) and recorded by a personal computer. The equation is given below:

$$C_B(t) = \frac{A}{V_B} \frac{DH}{L} C_A(t - t_0)$$

where D (cm²/s) is the diffusivity, H is the partition coefficient, L (cm) is the film thickness, A (cm²) is the surface area, V (ml) is the cell volume, C (wt%) is the methanol concentration, subscript "A" denotes the cell containing the water/methanol mixture, and subscript "B" the water cell. The product DH was obtained by extrapolating the experimentally measured data, and that value was considered to be the methanol permeability.

Membrane Preparation. Membranes were prepared by casting solutions of E-SFQK ionomer dissolved in DMAc on clean glass substrate. The concentration of the polymer solution was 30% (w/v), which allowed some control over the thickness of the membrane. The polymer solutions were filtered to remove particulates using a disposable syringe and disk filters (1 μm) prior to casting. Removal of DMAc was accomplished in an oven at 50 °C in an inert (N₂) environment over 3 h. The cross-linked membrane (CSFQK; potassium salt form of CSFQH) was placed on a hotplate with gradually increasing temperature from 50 to 200 °C over 1 h and at 250 °C for 100 min, while the noncross-linked membrane (NSFQK; potassium salt form of NSFQH) did not have any thermal treatment.

Membrane Acidification and Washing Conditions. Membranes were immersed in 1 M sulfuric acid (H₂SO₄) solution at room temperature for 24 h, followed by immersion in deionized water at room temperature for 24 h. All acidified membranes were stored at room temperature in deionized water for at least 5 days before testing.

Results and Discussion

Synthesis of SFQK and E-SFQK. The effect of reaction temperature on the inherent viscosities (η_{inh}) of E-SFQK was examined by 16 h of polymerization at 140, 145, and 155 °C. At a reaction temperature of 155 °C, the reacting solution formed a gel after benzene was removed as an azeotropic solvent. From ¹⁹F NMR spectra of E-SFQK, it can be seen that side reactions of E-SFQK occurred at the *ortho* position of decafluorobiphenyl (DFBP) at a reaction temperature of 155 °C, while there is no side reaction of DFBP at reaction temperatures of 140 and 145 °C. The effect of reaction time on the inherent viscosities (η_{inh}) of E-SFQK has been studied by varying reaction time from 1 to 20 h, keeping the reaction conditions such as monomer molar ratio, activation time of the hydroxy group of the SHQ monomer, and reaction temperature constant, with the latter at 140 °C (Figure 1). The reaction time of end capping of 3-ethynylphenol was also kept at 3 h. As shown in Figure 1, the polymerization is very fast and essentially complete after 7 h. This result indicated that the fluorine in the *para* position in DFBP is very reactive with activated SHQ. The inherent viscosities (η_{inh}) of E-SFQK were almost unchanged after 7 h of the polymerization reaction. The molecular weight (M_n) of E-SFQK was also measured from the relative ¹H NMR integrals of the proton in the ethynyl end group and the aromatic resonances. The molecular weights of E-SFQKs were over 15 kg mol⁻¹ after 7 h of polymerization (Table 2). Inherent viscosity

Table 2. Effect of Reaction Time on the Inherent Viscosities (η_{inh}) of E-SFQK

polymerization time (h)	η^a	η_{rel}^a	η_{inh} (dL/g) ^a	M_n^b	yield (%)
1	2.675	1.367	0.626	11 800	91
3	2.844	1.454	0.749	13 900	93
5	2.882	1.473	0.775	14 700	92
7	2.880	1.473	0.774	15 200	93
10	2.899	1.482	0.787	15 700	94
15	2.889	1.477	0.780	15 200	93
20	2.894	1.480	0.784	15 300	94

^a η , η_{rel} , and η_{inh} were measured at a concentration of 0.5 g/dL in DMAc for potassium form of E-SFQKs at 25 °C by using these equations. $\{\eta_{inh} = (\ln \eta_{rel})/C$ and $\eta_{rel} = \eta/\eta_0 = t/t_0$, where η_0 and C are the viscosity of DMAc ($\eta_0 = 1.956$) and the concentration of sulfonated polymer (0.5 g/dL), respectively.} ^b The molecular weights (M_n) of sulfonated polymers were calculated from the relative ¹H NMR integrals of the proton in the ethynyl end groups and the aromatic resonances.

measurement also supported a similar tendency with the end group analysis of NMR characterization.

The molecular structure of E-SFQK was characterized by ¹H NMR, ¹⁹F NMR, and FT-IR spectrum. All peaks shifted downfield in ¹H NMR spectra following polymerization due to replacement of hydrogen atoms by the perfluorophenylene group. Furthermore, all the peaks in the polymer spectra are broader than those of the monomers. ¹H NMR spectra of E-SFQK showed big three aromatic peaks at 7.53 (s), 7.31 (s), and 7.28 (s) ppm due to the SHQ moiety (Figure 2a). Subpeaks at 7.15 to 6.99 and 4.17 ppm were due to the ethynyl moiety. The ¹⁹F NMR spectrum of E-SFQK is dominated by peaks centered at -136.12 (dd) and -151.58 (dd) ppm, corresponding to *ortho* and *meta* fluorine atoms, respectively (Figure 2b). The fluorine peak related to the *para* position disappeared completely. The complete nucleophilic aromatic substitution was confirmed by the removal of *para* positioned fluorine atom in the ¹⁹F NMR spectra. E-SFQK was soluble in aprotic polar solvents such as DMSO, DMF, DMAc, and NMP (Table 1). This indicates that the E-SFQK was synthesized without side reaction. The FT-IR spectrum of E-SFQK shows sulfonate (SO₃) moiety peaks at 1019, 1189, and 1264 cm⁻¹, corresponding to the symmetric, asymmetric, and wagging peaks, respectively (Figure 3).

TG analysis of CSFQH and NSFQH membranes showed glass transitions at 307 and 303 °C, respectively, due mainly to a weight loss of sulfonic acid group (Figure 4). DSC analysis was performed to study the effect of cross-linking time on the glass transition temperature (T_g) of the membrane and to observe the exact time to cross-link the membrane. DSC curves showed that the glass transition temperature increased with increasing cross-linking time of the membrane (Figure 5). Additionally, an intense exothermic peak was seen as the reaction peak of ethynyl moiety.^{13b,c} This indicates that cross-linkable ethynyl groups of polymer chain ends react with each other around 250 °C, thus increasing cross-linking time of the membrane. After cross-linking the membrane for 100 min, this intense exothermic peak disappeared completely. The observed results were supported by the previously reported papers, which represented the changes for cross-linking of ethynyl moieties using the exothermic peaks and the glass transition temperature (T_g) observed by DSC analysis and using the ethynyl (acetylenic) C-H peak assignment around 3310 cm⁻¹ from FT-IR measurement during the curing process.^{13b,c,20} The T_g of CSFQH was observed at 247 °C, making it a possible candidate for a high temperature polymer electrolyte fuel cell. Low temperature stability was performed for liquid fuel cell application in the extremely low temperature region. In the test, dried and hydrated CSFQH membranes were very stable and flexible at -30 °C.

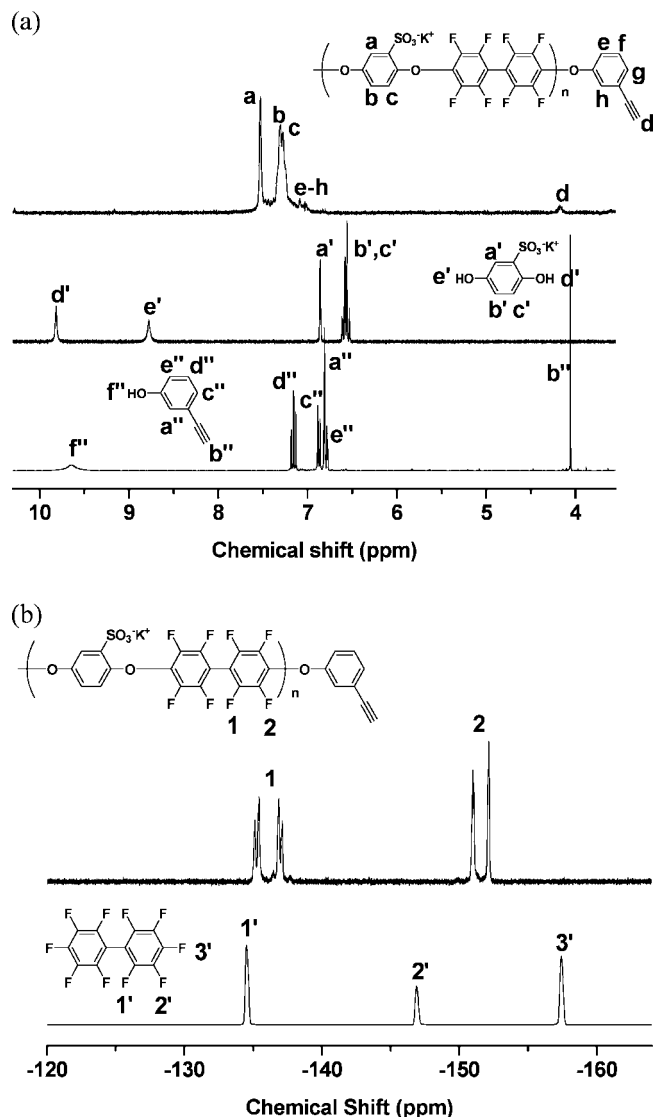


Figure 2. ^1H NMR (a) and ^{19}F NMR (b) spectra of E-SFQK.

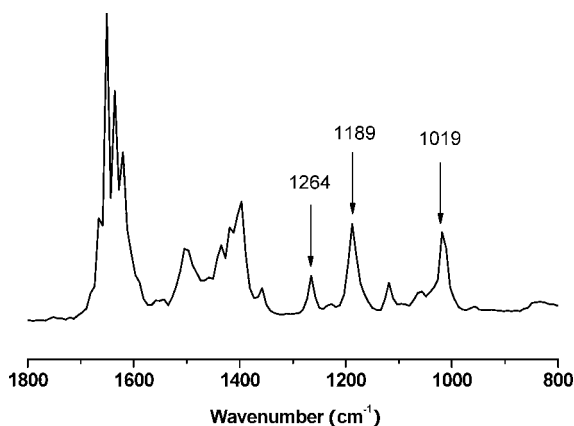


Figure 3. FT-IR spectrum of E-SFQK.

Effect of Cross-Linking Time on the Transport Properties. The effect of cross-linking time on the transport properties was investigated. Membranes were prepared, varying thermal-cross-link time from 0 to 100 min at 250 $^{\circ}\text{C}$. During this thermal curing processing of the membrane, the ethynyl group of the polymer chain end acts as a thermally cross-linkable moiety.^{13b,c} Proton conductivity, water uptake and swelling ratio of the membranes showed a similar tendency to decrease with increas-

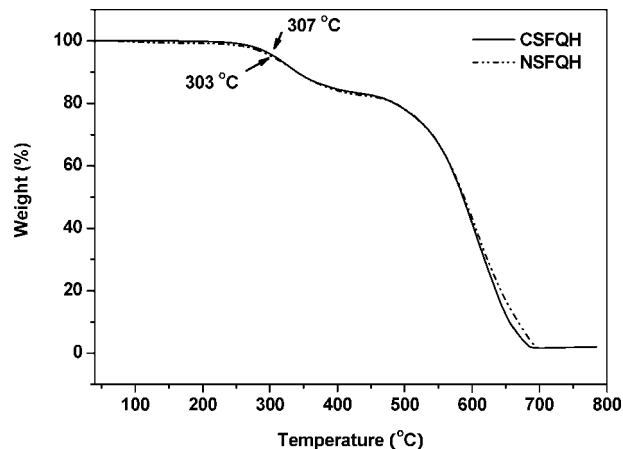


Figure 4. TG analysis of noncross-linked (NSFQH) and cross-linked (CSFQH) membranes.

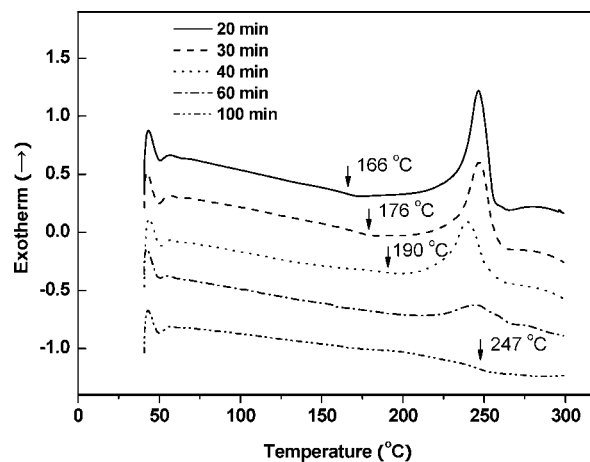


Figure 5. DSC curves of the effect of the degree of cross-linking on the glass transition temperature of membrane.

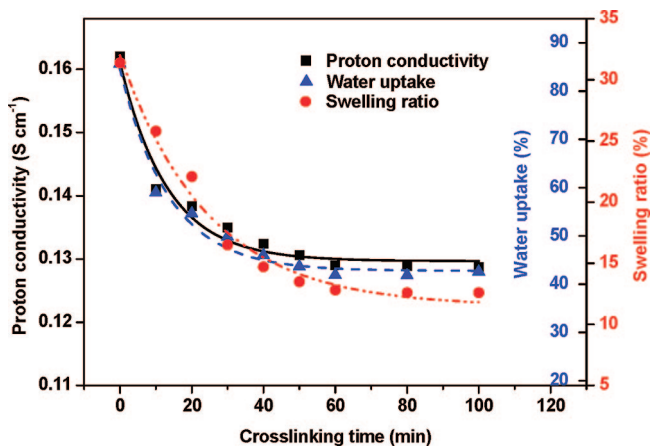
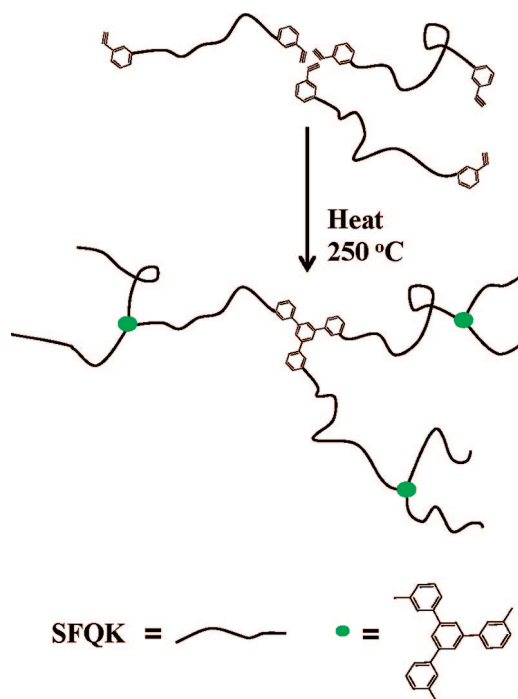


Figure 6. Effect of cross-linking time on proton conductivity (square), water uptake (triangle), and swelling ratio (circle) of membranes.

ing cross-linking time (Figure 6) and were in the range from 0.16 to 0.13 S cm^{-1} , 86% to 42%, and 31% to 13%, respectively, with increasing the cross-linking time. Proton conductivity of cross-linked membrane was 0.21 S cm^{-1} at 90 $^{\circ}\text{C}$, while that of noncross-linked membrane could not be measured because of the membrane cracking at 70 $^{\circ}\text{C}$. Critical changes in the transport properties occurred at 30 min of cross-linking time, and transport properties remained constant from 60 min onward. The main reason for these changes of transport properties is

Scheme 2. Thermal Cross-Linking Mechanism



related to the change of polymer structure during cross-linking reaction (Scheme 2). An earlier study of the McGrath group represented functionalized end-capped polyimide with ethynyl group at the end of the polymer. In the report, during thermal cross-linking of the ethynyl end-group, polymer structure gradually changed into a dense network structure.¹⁹ In this work, this result indicated that free volume of the polymer membrane decreased, and the size of the hydrophilic domain, which can contain water, was much affected from cross-linking. This structural change will be discussed with morphology study of AFM phase images of cross-linked and noncross-linked membrane in a later part of this paper.

Methanol Permeability and Selectivity. As can be seen in Table 3, the methanol permeability of NSFQH (noncross-linked membrane) could not be measured due to the solubility problem (Table 1). In this part of the study, our group therefore compared CSFQH (cross-linked membrane) to a state of the art Nafion membrane. CSFQH exhibited proton conductivity that was almost 1.4 times that of Nafion 117 (0.13 S/cm vs 0.09 S/cm). In addition, CSFQH also exhibited lower methanol permeability (88×10^{-8} cm²/s) than that of Nafion 117 (154×10^{-8} cm²/s). The high proton conductivity and low methanol permeability of CSFQH resulted in good selectivity as a polymer electrolyte membrane for direct methanol fuel cell. Selectivity was more than 2.5 times that of Nafion 117. However, water uptake was higher than that of Nafion 117. Although CSFQH had a high water uptake compared to Nafion, other properties such as proton conductivity and fuel cell selectivity exhibited good results (Table 3).

Chemical Resistance and Oxidative Stability. Chemical resistance of CSFQH and NSFQH membranes were measured

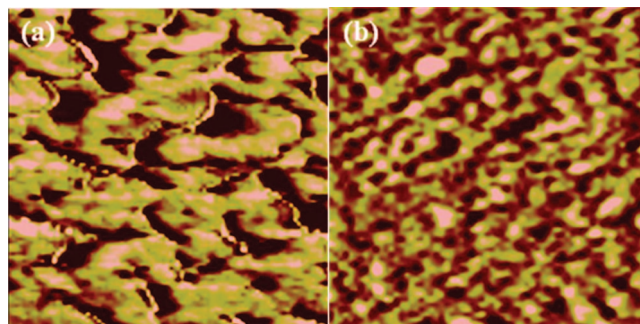


Figure 7. AFM tapping phase images of noncross-linked membrane (NSFQH) (z-scale 30) (a) and cross-linked membrane (CSFQH) (z-scale 7) (b). (Size is 500 nm × 500 nm.)

by testing membrane solubility in various common organic solvents. CSFQH was found to be insoluble in any organic solvent and to have very good chemical resistance, while NSFQH is very soluble in aprotic polar solvents such as DMAc, DMSO, NMP, and DMF. Additionally, in Fenton's test (3% H₂O₂ aqueous solution containing 2 ppm FeSO₄) at 80 °C, oxidative stability showed that the CSFQH membrane endured for 4 h before beginning to dissolve. Complete dissolution occurred only after more than 7 h. The NSFQH membrane only endured for 1 h 20 min before it started to dissolve. After over 2 h, the membrane had completely dissolved. These results indicated that the cross-linked membrane (CSFQH) had much better oxidative stability than the noncross-linked membrane (NSFQH). Additionally, CSFQH membrane exhibited relatively good oxidative stability compared to other membranes in previous reports.^{12a,21} Previously reported papers represented that fluorine containing groups are highly effective in improving oxidative stability of the sulfonated polymer membrane, and that a branched polymer membrane showed even better oxidative stability than the corresponding unbranched one with similar fluorine contents due to lower water uptake of branched polymer membrane.²¹ The branched polymer membrane endured for 4 h before beginning to dissolve (the dissolving time). In our work, introduction of the fluorine atoms of DFBP moieties as hydrophobic groups in the polymer main chain, along with the cross-linking system at the end of the polymer, prolonged the dissolving time and the dissolved time.

Morphological Study. As shown in the AFM phase images in Figure 7, the dark softer region indicate the hydrophilic sulfonic acid groups containing a large fraction of water, and the bright harder region indicate the hydrophobic fluorinated aromatic groups.^{4c,d,12e} In the aspect of two-dimensional surface morphology, dark regions in NSFQH membranes made channels of hydrophilic sulfonic acid groups containing water. The hydrophilic domain sizes of NSFQH were in the range of 20–50 nm, while dark regions of CSFQH membrane made clusters of hydrophilic domains whose sizes were in the range of 5–20 nm. These observations suggest that the free volume of the sulfonic acid groups, which is able to contain water, decreased after cross-linking. This effect demonstrated that the cross-linking between the polymer chains was well formed.

Table 3. Effect of Thermal Cross-Linking on the Proton Conductivity, Water Uptake, and Methanol Permeability of the Membrane

polymer membrane	IEC (mequiv/g)		water uptake (%)	conductivity (S/cm)		methanol permeability (10 ⁻⁸ cm ² /s)	Φ (10 ³ s Ω ⁻¹ cm ⁻³) ^a
	calcd	obsd		30 °C	90 °C		
CSFQH	2.07	2.04	42	0.13	0.21	88	148
NSFQH	2.07	2.06	86	0.16	<i>b</i>	<i>b</i>	<i>b</i>
Nafion 117	0.91	0.91	21	0.09	0.18	154	58

^a Φ (membrane selectivity): Proton conductivity to methanol permeability. ^b Can not detected or be measured.

Conclusions

Ethynyl-terminated sulfonated-fluorinated poly(arylene ether) was prepared for fuel cell applications. The cross-linkable end-group of the polymer acted not only to improve the thermal stability and dimensional stability of the membrane, but also to prolong the degradation time from radical attack. This cross-linked membrane structure, suggested as a network structure by a previous report,¹⁹ had low water uptake and swelling ratio with reasonable proton conductivity. Although CSFQH has lower proton conductivity than NSFQH, other properties of CSFQH, such as oxidative stability, chemical resistance, water uptake, and swelling ratio, were better than those of NSFQH. High proton conductivity and low methanol permeability of CSFQH resulted in better selectivity ($88 \times 10^{-8} \text{ cm}^2/\text{s}$) than that of Nafion 117 ($154 \times 10^{-8} \text{ cm}^2/\text{s}$). After cross-linking, the hydrophilic domain size decreased from the range of 20–50 nm to the range of 5–20 nm. These results indicate that CSFQH is a promising candidate for a polymer electrolyte for direct methanol fuel cells (DMFC) and high temperature polymer electrolyte fuel cells.

Acknowledgment. We thank Dr. Y. S. Kim for helpful discussions and comments. This work was supported in part by Plant Technology Advancement Program funded by the Ministry of Land, Transport and Maritime Affairs of the Government of Korea (#07seaHEROB02-03-01).

References and Notes

- (1) (a) Vielstich, W.; Lamm, A.; Gasteiger, H. A. *Handbook of Fuel Cells—Fundamentals, Technology and Applications*; John Wiley & Sons Ltd: Chichester, U.K., 2003. (b) Carratte, L.; Friedlich, K. A.; Stimming, U. *Fuel Cells* **2001**, 1, 5. (c) Steele, B. C. H.; Heinzel, A. *Nature* **2001**, 414, 345.
- (2) (a) Hickner, M. A.; Ghassemi, H.; Kim, Y. S.; Einsla, B. R.; McGrath, J. E. *Chem. Rev.* **2004**, 102, 4587. (b) Li, Q. F.; He, R. H.; Jensen, J. O.; Bjerrum, N. J. *Chem. Mater.* **2003**, 15, 4896. (c) Kreuer, K. D. *J. Membr. Sci.* **2001**, 185, 3. (d) Savadogo, O. *J. New Mater. Electrochem. Syst.* **1998**, 1, 47.
- (3) (a) Mauritz, K. A.; Moore, R. B. *Chem. Rev.* **2004**, 104, 4535. (b) Eisenberg, A.; Yeager, H. L. *Perfluorinated Ionomer Membranes*; ACS Symposium Series 180; American Chemical Society: Washington, DC, 1982. (c) Rikukawa, M.; Sanui, K. *Prog. Polym. Sci.* **2000**, 25, 1463.
- (4) (a) Wang, F.; Hickner, M.; Ji, Q.; Harrison, W.; Mechem, J.; Zawodzinski, T. A.; McGrath, J. E. *Macromol. Symp.* **2001**, 175, 387. (b) Miyatake, K.; Chikashige, Y.; Watanabe, M. *Macromolecules* **2003**, 36, 9691. (c) Kim, Y. S.; Wang, F.; Hickner, M.; McCartney, S.; Hong, Y. T.; Harrison, W.; Zawodzinski, T. A.; McGrath, J. E. *J. Polym. Sci., Part B: Polym. Phys.* **2003**, 41, 2816. (d) Kim, Y. S.; Hickner, M.; Dong, L.; Pivovar, B. S.; McGrath, J. E. *J. Membr. Sci.* **2004**, 243, 317. (e) Kim, Y. S.; Einsla, B.; Sankir, M.; Harrison, W.; Pivovar, B. S. *Polymer* **2006**, 47, 4026. (f) Einsla, M. L.; Kim, Y. S.; Hawley, M.; Lee, H. S.; McGrath, J. E.; Liu, B.; Guiver, M. D.; Pivovar, B. S. *Chem. Mater.* **2008**, 20, 5636.
- (5) (a) Gao, Y.; Robertson, G. P.; Guiver, M. D.; Mikhailenko, S. D.; Li, X.; Kaliaguine, S. *Macromolecules* **2004**, 37, 6748. (b) Kreuer, K. D. *J. Membr. Sci.* **2001**, 185, 29. (c) Jeong, M. H.; Lee, K. S.; Hong, Y. T.; Lee, J. S. *J. Membr. Sci.* **2008**, 314, 212.
- (6) (a) Fang, J. H.; Guo, X. X.; Harada, S.; Watari, T.; Tanaka, K.; Kita, H.; Okamoto, K. *Macromolecules* **2002**, 35, 9022. (b) Asano, N.; Aoki, M.; Suzuki, S.; Miyatake, K.; Uchida, H.; Watanabe, M. *J. Am. Chem. Soc.* **2006**, 128, 1762. (c) Genies, C.; Mercier, R.; Sillion, B.; Cornet, N.; Gebel, G.; Pineri, M. *Polymer* **2001**, 42, 359.
- (7) (a) Miyatake, K.; Iyotani, H.; Yamamoto, K.; Tsuchida, E. *Macromolecules* **1996**, 29, 6969. (b) Miyatake, K.; Shoyji, E.; Yamamoto, K.; Tsuchida, E. *Macromolecules* **1997**, 30, 2941.
- (8) Ghassemi, H.; Ndip, G.; McGrath, J. E. *Polymer* **2004**, 45, 5855.
- (9) (a) Wainright, J. S.; Wang, J.-T.; Weng, D.; Savinell, R. F.; Litt, M. *J. Electrochem. Soc.* **1995**, 142, L121. (b) Xing, B.; Savadogo, O. *J. New Mater. Electrochem. Syst.* **1999**, 2, 95.
- (10) (a) Bernardi, D. M.; Verbrugge, M. W. *J. Electrochem. Soc.* **1992**, 139, 2477. (b) Assink, R. A.; Arnold Jr., C.; Holladsworth, R. P. *J. Membr. Sci.* **1991**, 56, 143.
- (11) (a) Hübner, G.; Roduner, E. *J. Mater. Chem.* **1999**, 9, 409. (b) Curtin, D. E.; Lousenberg, R. D.; Henry, T. J.; Tangeman, P. C.; Tisack, M. E. *J. Power Sources* **2004**, 131, 41. (c) Panchenko, A. *J. Membr. Sci.* **2006**, 278, 269.
- (12) (a) Miyatake, K.; Zhou, H.; Matsuo, T.; Uchida, H.; Watanabe, M. *Macromolecules* **2004**, 37, 4961. (b) Kim, D. S.; Robertson, G. P.; Guiver, M. D.; Lee, Y. M. *J. Membr. Sci.* **2006**, 281, 111. (c) Lee, H. C.; Hong, H. S.; Kim, Y. M.; Choi, S. H.; Hong, M. Z.; Lee, H. S.; Kim, K. *Electrochim. Acta* **2004**, 49, 2315. (d) Miyatake, K.; Hay, A. S. *J. Polym. Sci., Part A: Polym. Chem.* **2001**, 39, 3211. (e) Ghassemi, H.; McGrath, J. E.; Zawodzinski, T. A. *Polymer* **2006**, 47, 4132.
- (13) (a) Hudlik, M. *Chemistry of Organic Fluorine Compounds*, 2nd ed.; Ellis Horwood: Chichester, U.K., 1992; 531–557. (b) Lee, K. S.; Lee, J. S. *Chem. Mater.* **2006**, 18, 4519. (c) Kim, J.-P.; Lee, W.-Y.; Kang, J.-W.; Kwon, S.-K.; Kim, J.-J.; Lee, J.-S. *Macromolecules* **2001**, 34, 7817.
- (14) (a) Kerres, J. A. *J. Membr. Sci.* **2001**, 185, 3. (b) Kerres, J. A. *Fuel Cells* **2005**, 5, 230.
- (15) (a) Kerres, J.; Ullrich, A.; Meier, F.; Häring, T. *Solid State Ionics* **1999**, 125, 243. (b) Kosmala, B.; Schauer, J. *J. Appl. Polym. Sci.* **2002**, 85, 1118. (c) Gao, Y.; Robertson, G. P.; Guiver, M. D.; Jian, X.; Mikhailenko, S. D.; Kaliaguine, S. *Solid State Ionics* **2005**, 176, 409.
- (16) (a) Kerres, J.; Cui, W.; Junginger, M. *J. Membr. Sci.* **1998**, 139, 227. (b) Mikhailenko, S. D.; Wang, K.; Kaliaguine, S.; Xing, P.; Robertson, G. P.; Guiver, M. D. *J. Membr. Sci.* **2004**, 233, 93.
- (17) Chikashige, Y.; Chikyu, Y.; Miyatake, K.; Watanabe, M. *Macromol. Chem. Phys.* **2006**, 207, 1334.
- (18) (a) Zhong, S.; Cui, X.; Cai, H.; Fu, T.; Zhao, C.; Na, H. *J. Power Sources* **2007**, 164, 65. (b) Heo, K. B.; Lee, H. J.; Kim, H. J.; Kim, B. S.; Lee, S. Y.; Cho, E.; Oh, I. H.; Hong, S. A.; Lim, T. H. *J. Power Sources* **2007**, 172, 215.
- (19) (a) Moy, T. M.; DePorter, C. D.; McGrath, J. E. *Polymer* **1993**, 34, 819. (b) Jayaraman, S.; Srinivasan, R.; McGrath, J. E. *J. Polym. Sci., Part A: Polym. Chem.* **1995**, 33, 1551.
- (20) Lee, H. J.; Lee, M. H.; Oh, M. C.; Ahn, J. H.; Han, S. G. *J. Polym. Sci., Part A: Polym. Chem.* **1999**, 37, 2355.
- (21) (a) Miyatake, K.; Asano, N.; Watanabe, M. *J. Polym. Sci., Part A: Polym. Chem.* **2003**, 41, 3901. (b) Miyatake, K.; Zhou, H.; Watanabe, M. *Macromolecules* **2004**, 37, 4956. (c) Asano, N.; Miyatake, K.; Watanabe, M. *Chem. Mater.* **2004**, 16, 2841. (d) Miyatake, K.; Chikashige, Y.; Watanabe, M. *Macromolecules* **2004**, 36, 9691.

MA802233J